Biomass Conversion and Biorefinery (2020) 10:523–533
https://doi.org/10.1007/s13399-019-00447-9

ORIGINAL ARTICLE

A detailed study of pyrolysis conditions on the production of steam-activated carbon derived from oil-palm shell and its application in phenol adsorption

Aik Chong Lua[1]

Received: 8 March 2019 / Revised: 20 May 2019 / Accepted: 21 May 2019 / Published online: 11 June 2019

Abstract
Oil-palm shell, a biomass waste from the palm oil industry, can be converted into commercially viable activated carbon through pyrolysis, followed by activation. A detailed systematic study of the pyrolysis conditions and initial shell particle size was conducted, and they were found to have significant effects on the pore characteristics of steam-activated carbons. The optimum pyrolysis conditions were (i) pyrolysis temperature of 750 °C, hold time of 2 h, heating rate of 10 °C/min, nitrogen flow rate of 150 cm^3/min and particle size range of 2–2.8 mm for pyrolysis in nitrogen flow, and (ii) pyrolysis temperature of 675 °C, hold time of 2 h, heating rate of 10 °C/min and particle size range of 2–2.8 mm for pyrolysis under vacuum. Under nitrogen pyrolysis environment, the best activated carbon yielded the highest BET surface area of 794 m^2/g and achieved the largest adsorption capacity of 129 mg of phenol per g of activated carbon. Under vacuum pyrolysis, the best activated carbon yielded the highest BET surface area of 988 m^2/g and achieved the largest adsorption capacity of 168 mg of phenol per g of activated carbon which was respectively 24% and 30% greater than those for the activated carbon pyrolysed in nitrogen flow. Of all pyrolysis parameters studied—pyrolysis temperature, hold time, heating rate (low heating rate region), nitrogen flow rate, shell particle size and pyrolysis environment—the pore characteristics of the steam-activated carbons are strongly dependent on the pyrolysis temperature, hold time, pyrolysis environment and initial particle size.

Keywords Oil-palm shell · Pyrolysis · Pore surface area · Steam-activated carbon · Phenol adsorption

1 Introduction

Activated carbon is commonly used as an adsorbent to mitigate gaseous pollutants and remove dissolved impurities in potable water, groundwater, waste streams and other aqueous sources. In gaseous pollution, activated carbon can be used as an adsorbent to remove hydrogen sulphide [1], sulphur dioxide [2], ammonia [3] and volatile organic compounds such as toluene and chlorobenzene [4] which may be emitted from sewage treatment plants, chemical industries and oil refineries. Guo et al. [1] conducted hydrogen sulphide (H_2S) adsorption experiments in a fixed bed of oil-palm shell activated carbons and reported adsorption capacities of 46, 68 and 76 mg of H_2S per g of activated carbons prepared by CO_2, KOH and H_2SO_4 activation, respectively. Guo and Lua [2] reported adsorption capacities of 76 and 63 mg of SO_2 per g of oil-palm shell activated carbons impregnated with 10% KOH and 30% H_3PO_4, respectively. Guo et al. [3] reported that adsorption of NH_3 onto palm shell activated carbons impregnated with H_2SO_4 increased with physisorption as well as chemisorption which is due to its surface oxygen functional groups. Zhao et al. [4] prepared coconut shell–derived activated carbon which produced better adsorption removal of toluene and chlorobenzene than a commercial coal activated carbon. In aqueous applications, waste effluents from coal preparation plants, mineral mining and processing industries, textile mills, paper mills, tanneries, petrochemical industries and electroplating plants contain toxic heavy metals which can be removed by adsorption into activated carbons [5]. Industrial dye discharges from the textile, paper product, paint

✉ Aik Chong Lua
maclua@ntu.edu.sg

[1] School of Mechanical and Aerospace Engineering, Nanyang Technological University, 50 Nanyang Avenue, Singapore 639798, Republic of Singapore

and plastic industries are present in their effluent streams and are harmful to humans if ingested, and hence, activated carbons are used to remove these coloured dyes [6]. Phenolic compounds and their derivatives from petroleum refineries, plastic industries, coal carbonization and tar distillation units, phenol-formaldehyde plants, textile mills and pharmaceutical industries, and the large-scale agriculture use of pesticides can enter into the water resources and pose health concerns to humans. Adsorption of these carcinogenic compounds by activated carbons is an effective method to limit its ingress by humans [7].

Commercial activated carbons are prepared from a variety of carbonaceous raw materials. Presently, lignite, peat, wood and coconut shell are the main common precursors for commercial activated carbons. Studies reported in the literature on the preparation of activated carbons from agricultural wastes included oil-palm shell [7]; almond shell and hazelnut shell [8]; coconut shell [9]; walnut shell and olive stone [10]; peach stone [11]; apricot stone, cherry stone and grape seed [12]; eucalyptus kraft lignin [13]; pistachio-nut shell [14]; peanut shell [15]; date stone [16]; and oil-palm waste [17].

Activated carbon is usually produced in two stages—firstly a pyrolysis process and then followed by an activation process. In the pyrolysis process, thermal decomposition of the raw material is carried out under an inert gas or vacuum condition to produce char with rudimentary pore structure. Subsequently, the char is subjected to carbon dioxide or steam under a moderate to high temperature to produce activated carbon with well-developed pore structure. The pyrolysis operating conditions have effects on the pore development of the final activated carbon. Lua et al. [18] studied the influence of pyrolysis conditions on the pore development of activated carbons prepared from oil-palm shell. Nitrogen and carbon dioxide were used as gas streams in the pyrolysis and activation processes, respectively. With the chars subjected to fixed activation conditions, the optimum conditions for pyrolysis were a temperature of 600 °C, hold time of 2 h, nitrogen flow rate of 150 cm^3/min and heating rate of 10 °C/min. Lua and Yang [14] studied the effects of vacuum pyrolysis conditions on the characteristics of activated carbons derived from pistachio-nut shells. Experimental results showed that the activated carbon pyrolysed under a temperature of 500 °C, a hold time of 2 h and a heating rate of 10 °C/min had the highest BET surface area and micropore volume of 896 m^2/g and 0.237 cm^3/g, respectively. Liu et al. [19] studied the effects of pyrolysis conditions on the physicochemical structure of activated carbon derived from bituminous coal and found that pyrolysis under nitrogen flow at 800 °C and a residence time of 40 min were the most suitable for subsequent activation in carbon dioxide flow.

In this work, the effects of different pyrolysis operating conditions on the steam-activated carbons derived from oil-palm shells were studied. The complete pyrolysis conditions investigated were temperature, hold time, inert gas flow rate and heating rate. In addition, vacuum or reduced pressure pyrolysis, i.e. with no inert gas flow, was also studied. The effect of initial or raw shell particle size before pyrolysis was also investigated. The steam activations conditions were fixed whilst the pyrolysis parameter was varied one at a time. Adsorption studies were also carried out to determine the effectiveness of the steam-activated carbons to adsorb phenol in the aqueous state.

2 Experimental

2.1 Pyrolysis, activation and characterization

The raw oil-palm shells were crushed into smaller pieces and sieved to a size range of 1–6.3 mm. The shells were dried in an electrical oven at 110 °C for 24 h. During pyrolysis, approximately 20 g of shells was placed on a 120-μm metal mesh in a vertical stainless steel reactor (32 mm i.d. and 190 mm long) which was placed in an electrical furnace (Fig. 1). Nitrogen gas of 99.9995% purity, at room temperature of 25 °C and atmospheric pressure of 760 mmHg, flowed through the reactor at a pre-determined flow rate (50–250 cm^3/min) to provide an inert environment. The temperature in the reactor was measured by a thermocouple which was connected to a temperature controller. For pyrolysis under vacuum with no nitrogen gas flow, another vertical stainless steel reactor (57 mm i.d. and 400 mm long) which was connected to a mechanical pump was used to replace the reactor in Fig. 1 but with the nitrogen gas cylinder disconnected. During pyrolysis for both nitrogen and vacuum conditions, the furnace temperature was increased at a fixed heating rate (5–40 °C/min) from room temperature to a pre-determined temperature (400–900 °C) and held at this temperature for a length of time (0.5–3.0 h). Subsequently, the resulting chars were removed and placed into another reactor (18 mm i.d. and 330 mm long) to replace the reactor in Fig. 1 for steam

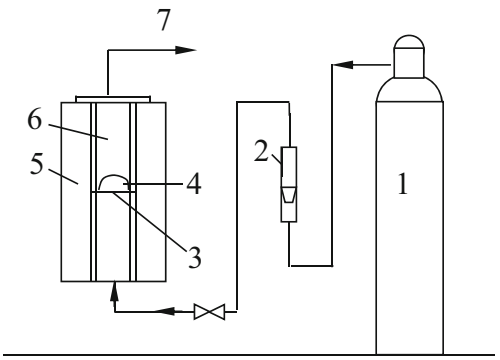

Fig. 1 Pyrolysis system for char preparation. (1) Gas cylinder, (2) gas volume flow meter, (3) metal mesh, (4) sample, (5) furnace, (6) reactor, (7) exhaust line

activation. This reactor was first connected to a nitrogen gas cylinder and then later replaced by an electric steam generator. All the chars were subjected to the same activation conditions. During activation, the chars were first heated under nitrogen flow (150 cm^3/min) from room temperature to 900 °C at a heating rate of 10 °C/min. Having reached the set temperature of 900 °C, nitrogen flow was terminated and steam from an electric steam generator was introduced. The steam flow rate was 1.4 kg/h at a pressure of 2.1×10^5 N/m^2, and the hold time during steam activation was 1 h. The resulting activated carbons were characterized using an accelerated surface area and porosimetry system (ASAP 2010, Micromeritics) under N_2 adsorption at −196 °C. Using the Brunauer-Emmett-Teller (BET) equation, data from the isotherms were used to determine the BET surface area. The t-plot method was used to calculate the micropore volume and the non-micropore surface area. The total pore volume was estimated to be the liquid volume of adsorbate (N_2) at a relative pressure of 0.985. The difference between the BET surface area and the non-micropore surface area is the micropore surface area.

2.2 Aqueous phase adsorption

Phenol GR (Merck & Co.) was used as the adsorbate for the adsorption studies. Fifty millilitres of phenol solution with a concentration of 200 mg/l was poured into a 125-ml conical flask. A weighed amount of activated carbon (8.4–65.1 mg) was added into the flask. The activated carbon was washed with boiling deionized water and subsequently dried at 110 °C for 24 h before use. The flask was placed in a shaker bath maintained at 30 °C and operating at a rotational speed of 150 rpm for 168 h. By measuring the phenol solution concentration before and after the adsorption test, the amount of phenol adsorbed by the activated carbons could be ascertained. The phenol concentration was measured by a gas chromatograph–mass spectrometer (6890N GC-5973MSD system, Agilent).

3 Results and discussion

3.1 Pore surface area and pore volume of steam-activated carbons

The effects of pyrolysis operating conditions and initial shell particle size on the BET surface area, micropore surface area and total pore volume of the final activated carbons were studied. After pyrolysis, all the chars were subsequently activated in steam under the same activation conditions.

The effect of pyrolysis temperature on the pore characteristics of the steam-activated carbons, pyrolysed in nitrogen flow, is shown in Fig. 2. Increasing the pyrolysis temperature from 400 to 650 °C, the BET surface area, micropore surface area and total pore volume of the activated carbons increased to a peak at 500 °C and thereafter decreased progressively until 650 °C. The initial increasing trend from 400 to 500 °C coincided with the release of the low-molecular-weight volatiles from the carbon structure as shown in the derivative thermogram (10 K/min heating rate) for pyrolysis of the oil-palm shells [20]. The evolution of the volatiles resulted in the rudimentary pore development in the chars, and subsequent steam activation of these chars enhanced the pore development and further increased new pores, resulting in increasing BET surface area, micropore surface area and total pore volume of the activated carbons for increasing pyrolysis temperature. However, for further increases in pyrolysis temperature from 500 to 650 °C, the BET surface area, micropore surface area and total pore volume of the steam-activated carbons progressively decreased with increasing pyrolysis temperature. This phenomenon could be attributed to the softening and melting of some of the remaining volatiles in the chars, resulting in the formation of an intermediate melt in the chars. Such evidence of an intermediate melt in the char had been reported by Lua and Yang [14]. The melt had partially closed some of the pores in the char, thereby obstructing the rudimentary pore structure development in the char. In the subsequent activation, the less well-developed pore structure in the char resulted in a lower steam-carbon reaction and reduced pore enhancement. Hence, the pore development in the activated carbons decreased progressively for increasing pyrolysis temperature from 500 to 650 °C. However, further increases in the pyrolysis temperature from 650 to 750 °C progressively enhanced the pore development of the activated carbons. Above 650 °C, depolymerization set in and the intermediate melt in the char commenced to volatilize which then opened up the pores previously closed by the melt. The volatilization was completed at 750 °C when the melt was cleared. The disappearance of the melt was observed by Lua and Yang [14]. Besides the opening of previously closed pores, new pores were formed due to the release of the high-molecular-weight volatiles for increasing pyrolysis temperature from 650 to 750 °C. Steam activation of these chars, pyrolysed from 650 to 750 °C, resulted in increasing BET surface area, micropore area and total pore volume with increasing pyrolysis temperature, peaking at 750 °C with BET surface area, micropore surface area and total pore volume values of 794 m^2/g, 637 m^2/g and 0.41 cm^3/g, respectively. Further increasing pyrolysis temperature from 750 to 900 °C resulted in decreasing BET surface area, micropore surface area and total pore volume of the activated carbons. At these high pyrolysis temperatures, shrinkage of the pore structure of the char and narrowing of the pore entrances occurred, resulting in a reduction of the accessible pore surface area of the char. Another possible reason is the formation of a secondary melt in the char arising from the high-molecular-weight volatiles, which is similar to the intermediate melt as discussed earlier. These then led to a decrease in the diffusion

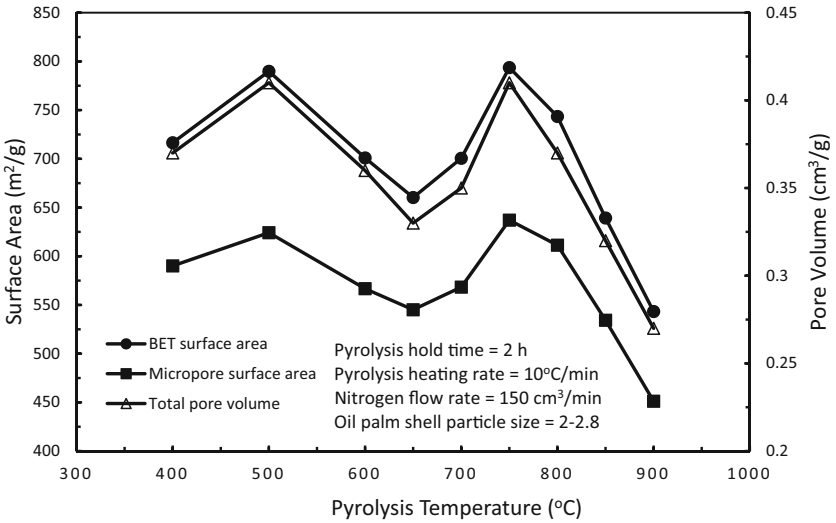

Fig. 2 Effect of pyrolysis temperature on the pore characteristics of activated carbons pyrolysed in nitrogen flow

of the steam molecules for the steam-carbon reaction during the subsequent steam activation process, and hence, increasing pyrolysis temperature from 750 to 900 °C continuously decreased the BET surface area, micropore surface area and total pore volume of the activated carbons.

Figure 3 shows the effect of pyrolysis temperature on the pore characteristics of activated carbons pyrolysed under vacuum condition. For the pyrolysis temperature range from 400 to 650 °C, the trends are generally similar to those for the activated carbons pyrolysed in nitrogen flow in Fig. 2 except that the surface areas and total pore volume started to increase at a lower pyrolysis temperature of 600 °C for the vacuum pyrolysis instead of 650 °C for the nitrogen pyrolysis. The intermediate melt appeared to commence its volatilization earlier, at 600 °C, and it was completely cleared away at 675 °C for the vacuum pyrolysis case instead of 750 °C for the nitrogen pyrolysis case. At 675 °C, the BET surface area peaked at 988 m^2/g which is 24% greater than that for the nitrogen pyrolysis case. Increasing pyrolysis temperature from 675 to 900 °C generally decreased the BET surface area, micropore surface area and total pore volume continuously except at 800 °C in which there was a slight upward trend. This general decreasing trend in the surface areas and total pore volume was due to the formation of a secondary melt and shrinkage of pore structure which was similar to the nitrogen pyrolysis results mentioned earlier. However, at 800 °C, the secondary melt in the char might have disappeared, leaving more pores for subsequent steam activation and hence an increase in pore development in the activated carbon. Thereafter, the overriding factor in reducing pore development for increasing pyrolysis temperature from 800 to 900 °C was due to the shrinkage of pore structure at these high pyrolysis temperatures.

A comparison between the results in Figs. 2 and 3 revealed that the vacuum-pyrolysed chars always yielded activated carbons with higher BET surface area, micropore surface area and total pore volume for the same pyrolysis temperature. Further, the release of the high-molecular-weight volatiles from the oil-palm shells, and the removal of the intermediate and secondary melts from the chars occurred at lower

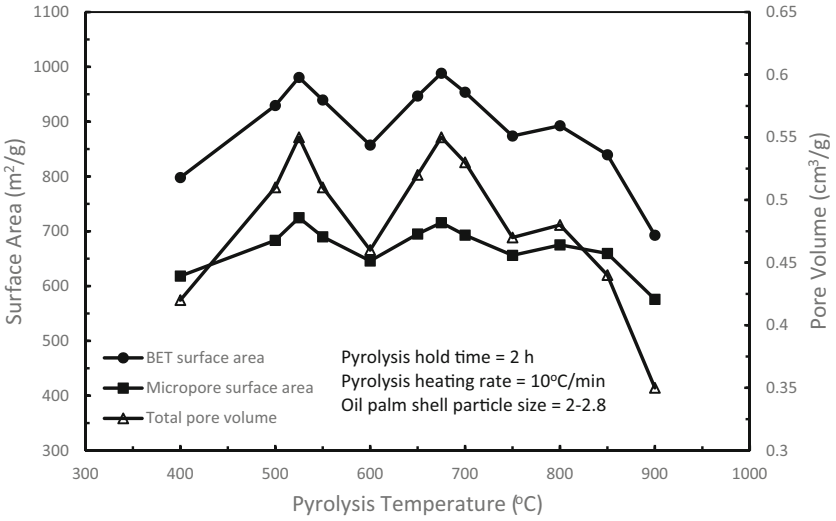

Fig. 3 Effect of pyrolysis temperature on the pore characteristics of activated carbons pyrolysed under vacuum condition

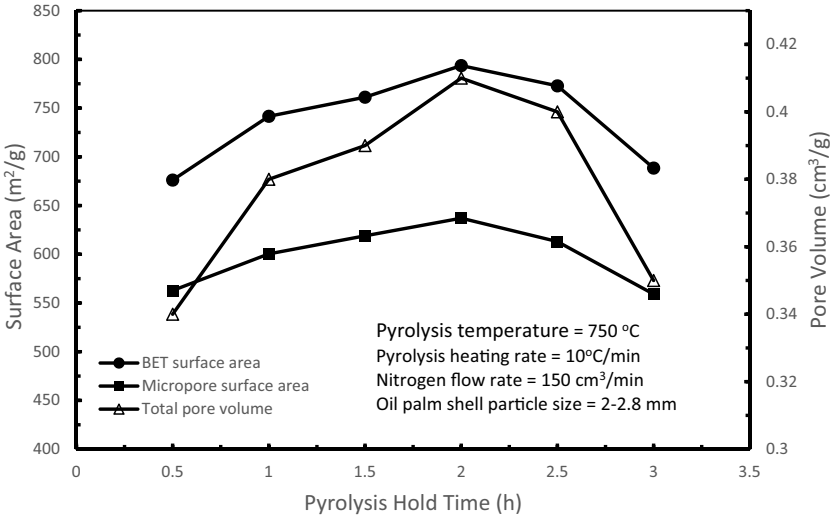

Fig. 4 Effect of pyrolysis hold time on the pore characteristics of activated carbons pyrolysed in nitrogen flow

pyrolysis temperatures for vacuum pyrolysis than those for nitrogen pyrolysis. This should also apply to the commencement of the low-molecular-weight volatile release if pyrolysis temperatures below 400 °C were available. From these results, it can be concluded that the depolymerization of volatiles in the oil-palm shell during pyrolysis is a function of both the pyrolysis temperature and pressure. Under vacuum pyrolysis, the near-zero pressure force enables the ease of vaporization of the volatiles throughout the entire pore structure of the oil-palm shell particle, forming a more well-defined rudimentary pore structure than that for nitrogen pyrolysis, and therefore yielding higher surface areas and total pore volume for vacuum-pyrolysed, steam-activated carbons. From the results presented in Figs. 2 and 3, the best pyrolysis temperatures to obtain the best pore characteristics in the resulting activated carbons were 750 and 675 °C for the nitrogen flow and vacuum pyrolysis cases respectively. These pyrolysis temperatures were used in the subsequent tests for studying other pyrolysis parameters.

The effect of pyrolysis hold time on the pore characteristics of the steam-activated carbons, pyrolysed in nitrogen flow, is shown in Fig. 4 for 0.5-, 1-, 1.5-, 2-, 2.5- and 3-h hold times. Increasing pyrolysis hold time from 0.5 to 2 h resulted in increasing release of both the low-molecular-weight and high-molecular-weight volatile matters, thereby forming increasing rudimentary pore structure within the chars, and hence increasing BET surface area, micropore surface area and total pore volume of the activated carbons upon subsequent steam activation, with the best pore characteristics at a pyrolysis hold time of 2 h. However, beyond 2-h hold time, the pore characteristics of the activated carbons commenced to deteriorate with increasing hold time from 2 to 3 h. Prolonged heat treatment during pyrolysis at 750 °C for these long hold times would lead to the softening and melting of the residual high-molecular-weight volatile matter, resulting in closing and sealing off part of the pore structure of the char, and possibly shrinkage of the pore structure at excessive long hold time of 3 h. All these led to reducing steam-carbon reaction during

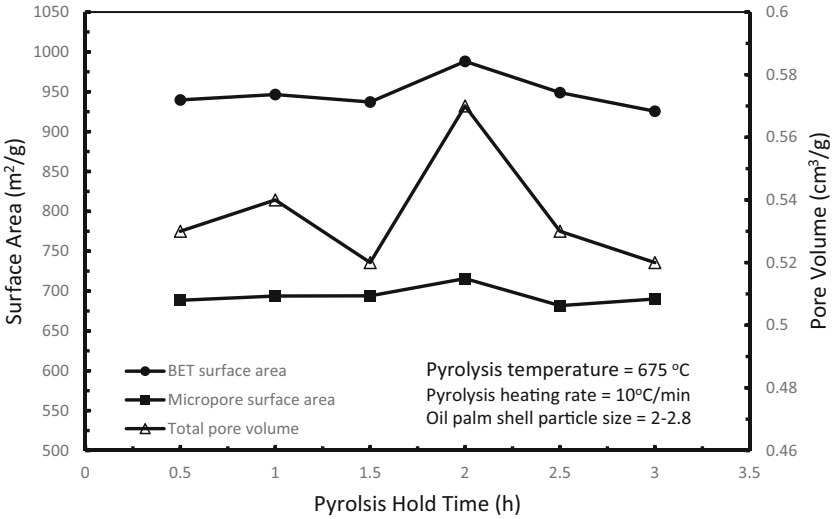

Fig. 5 Effect of pyrolysis hold time on the pore characteristics of activated carbons pyrolysed under vacuum condition

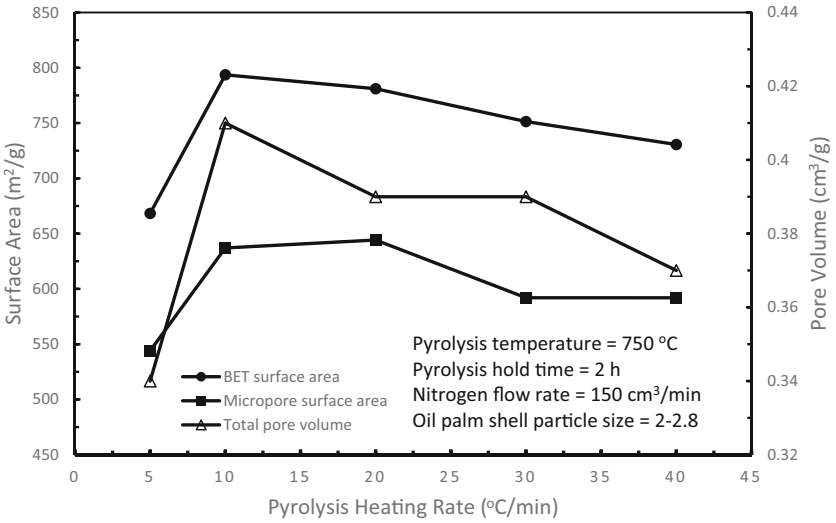

Fig. 6 Effect of pyrolysis heating rate on the pore characteristics of activated carbons pyrolysed in nitrogen flow

activation and hence reducing BET surface area, micropore surface area and total pore volume of the steam-activated carbons for increasing pyrolysis hold time from 2 to 3 h. Figure 5 shows the effect of pyrolysis hold time on the pore characteristics of the steam-activated carbons, pyrolysed under vacuum, for the same 0.5 to 3-h hold time as in Fig. 4. The pore characteristics of the steam-activated carbons remained relatively the same for increasing hold time from 0.5 to 1.5 h, indicating just 0.5-h hold time was required to release all the possible volatiles for this time span. At 2-h hold time, slight peaks in BET surface area, micropore surface area and total pore volume were observed and it is surmised that 2-h hold time was sufficient to release most of the low-molecular-weight and high-molecular-weight volatiles from the char. Consequently, the presence of a secondary melt, unlike the nitrogen pyrolysis results in Fig. 4, did not appear to be in play for hold times greater than 2 h. The marginal dips in the BET surface area, micropore surface area and total pore volume for hold times greater than 2 h could possibly be due to the slight shrinkage of the pore structure in the chars which were starting to occur for these longer hold times. Overall, a pyrolysis hold time of 2 h yielded the best BET surface area, micropore surface area and total pore volume of the steam-activated carbons under both nitrogen flow and vacuum pyrolysis, and therefore, a hold time of 2 h was used in the subsequent tests for studying other pyrolysis parameters.

The effect of heating rate during pyrolysis on the pore characteristics of the steam-activated carbons, pyrolysed in nitrogen flow, is shown in Fig. 6. Increasing pyrolysis heating rate from 5 to 10 °C/min increased the BET surface area, micropore surface area and total pore volume. After peaking at 10 °C/min, the BET surface area and total pore volume gradually decreased for increasing heating rate from 10 to 40 °C/min. For the micropore surface area, its peak was at 20 °C/min and then a general decreasing trend for increasing heating rate from 20 to 40 °C/min. The heating rate will directly impact on the temperature ramp-up time from room temperature to the final pyrolysis temperature

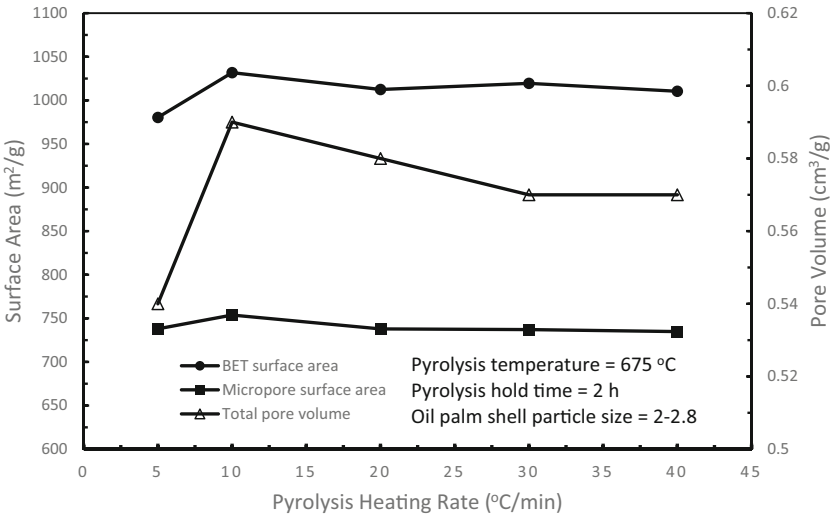

Fig. 7 Effect of pyrolysis heating rate on the pore characteristics of activated carbons pyrolysed under vacuum condition

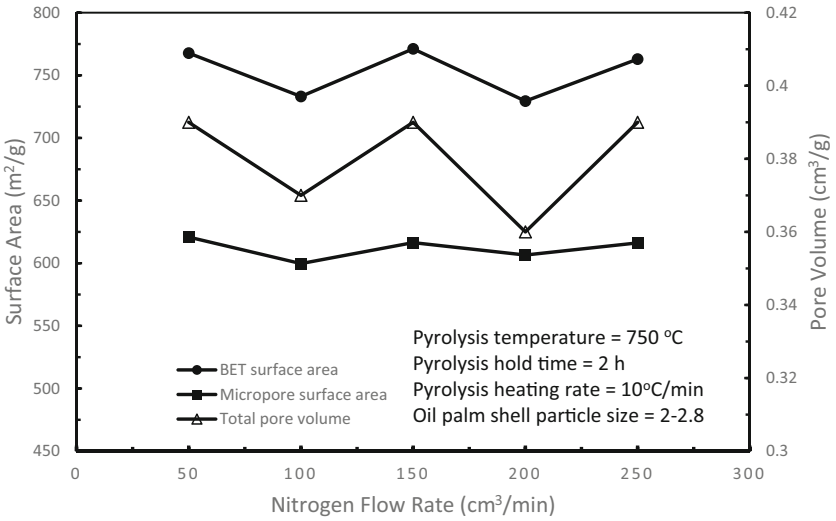

Fig. 8 Effect of nitrogen flow rate on the pore characteristics of activated carbons pyrolysed in nitrogen flow

and hence its effect on the residence time of the char during pyrolysis. Increasing the pyrolysis heating rate reduces the temperature ramp-up time from room temperature to the final pyrolysis temperature in the reactor and vice versa. For instance, increasing the heating rate from 5 to 10 °C/min decreased the temperature ramp-up time from 2.4 to 1.2 h. Hence, reducing the heating rate from 10 to 5 °C/min in Fig. 6 was tantamount to subjecting the char to the detrimental effects of the formation of a secondary melt and shrinkage of pore structure due to prolonged hold time as discussed earlier for the results in Fig. 4. Hence, this effect could be correlated to the decrease in the BET surface area, micropore surface area and total pore volume with decreasing pyrolysis heating rate from 10 to 5 °C/min. Increasing pyrolysis heating rate from 10 to 40 °C/min decreased the BET surface area and total pore volume (the micropore surface area showed decreasing trend after 20 °C/min) due to decreasing residence time and therefore reducing the amount of volatiles released. This had the effect of diminishing rudimentary pore structure in the char and hence decreasing BET surface area, micropore surface area and total pore volume in the subsequent activated carbons. Increasing the heating rate from 10 to 40 °C/min decreased the temperature ramp-up time, and therefore, the residence time decreased from 1.2 to 0.3 h. Figure 7 shows the effect of pyrolysis heating rate on the pore characteristics of the steam-activated carbons, pyrolysed under vacuum, for the same heating rates of 5 to 40 °C/min as in Fig. 6. Decreasing the heating rate from 10 to 5 °C/min increased the temperature ramp-up time and hence the residence time in the reactor, resulting in the decrease of BET surface area, micropore surface area and total pore volume of the steam-activated carbons due to the shrinkage of pore structure in the char as similarly observed for prolonged hold time (2 to 3 h) in Fig. 5. A pyrolysis heating rate of 10 °C/min resulted in a small peak in the pore characteristics of the activated carbon since, at this heating rate, it was sufficient to release most of the low-

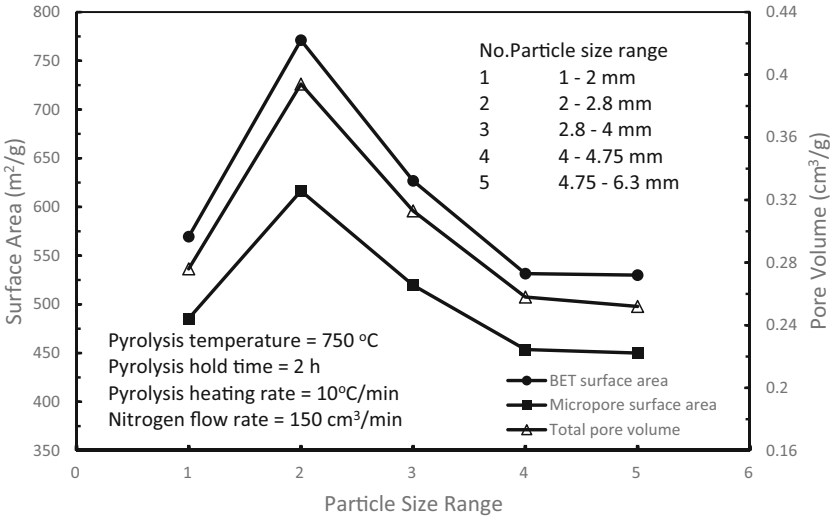

Fig. 9 Effect of particle size on the pore characteristics of activated carbons pyrolysed in nitrogen flow

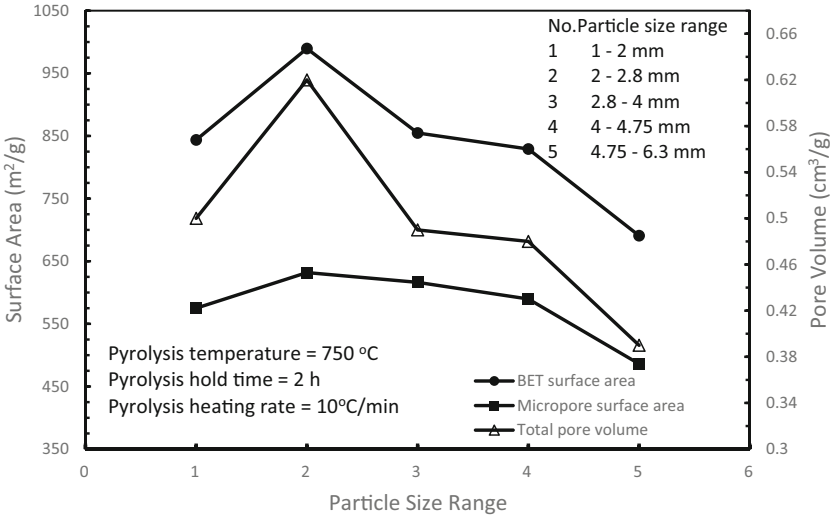

Fig. 10 Effect of particle size on the pore characteristics of activated carbons pyrolysed under vacuum condition

molecular-weight and high-molecular-weight volatiles from the char. Increasing the pyrolysis heating rate from 10 to 40 °C/min produced almost identical BET surface area, micropore surface area and total pore volume in the steam-activated carbons for all these pyrolysis heating rates even though the temperature ramp-up time had decreased from 1.08 to 0.27 h. This trend is similar to the pyrolysis hold time of 0.5 to 1.5 h in Fig. 5. The heating rates of 5 to 40 °C/min used in the pyrolysis of oil-palm shells are considered as low and therefore generally do not affect the reaction rate of the depolymerization process or the release of volatiles from the oil-palm shell structure. From the results of the heating rates for pyrolysis in nitrogen flow (Fig. 6) and under vacuum (Fig. 7), a pyrolysis heating rate of 10 °C/min was used in the subsequent tests for studying other pyrolysis parameters.

Figure 8 shows the effect of nitrogen flow rate on the pore characteristics of the steam-activated carbons when nitrogen was used the inert gas during the pyrolysis of the oil-palm shells in the reactor. Varying nitrogen flow rates did not have any significant effects on the BET surface area, micropore surface area and total pore volume. However, a flow rate of 150 cm^3/min produced a slightly better BET surface area in the steam-activated carbon than the rest of the flow rates. Hence, a nitrogen flow rate of 150 cm^3/min was used in the subsequent tests for studying the next pyrolysis parameter. The functions of the nitrogen purge gas during pyrolysis are to provide an inert atmosphere during the reaction and to remove any released volatile matter out of the reactor. In the results shown in Fig. 8, it is surmised that a nitrogen flow rate of 50 cm^3/min was sufficient to remove and entrain the volatiles in the nitrogen flow and out of the reactor. This would prevent the released volatiles from depositing on the char surfaces and blocking the pore entrances which would hinder further pore development in the char.

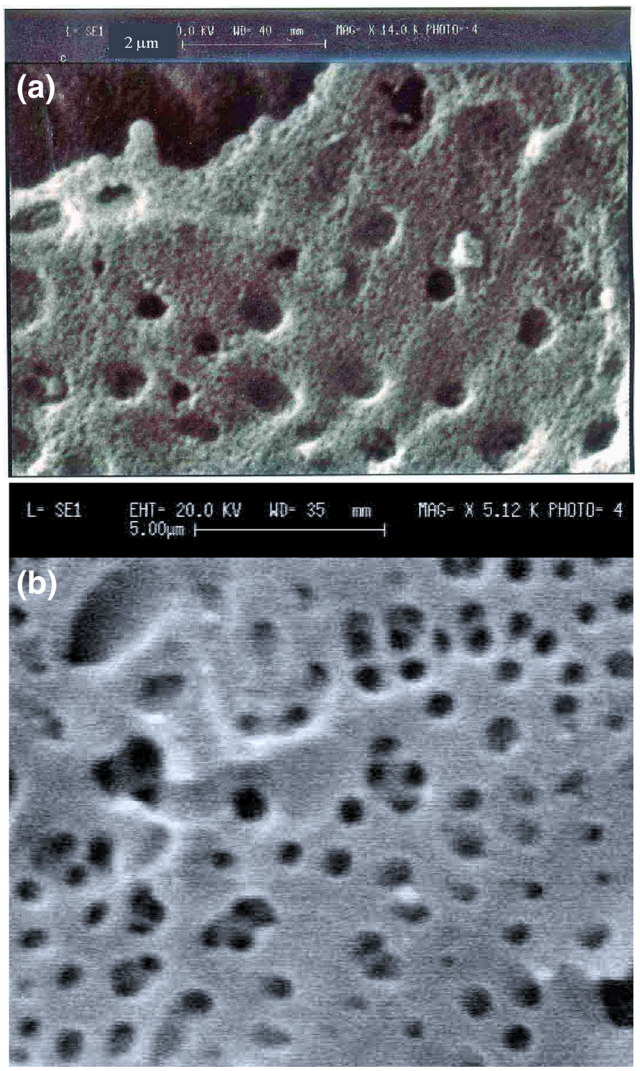

Fig. 11 Scanning electron micrographs of the surface morphology of activated carbon pyrolysed **a** in nitrogen (× 14,000), and **b** under vacuum (× 5120)

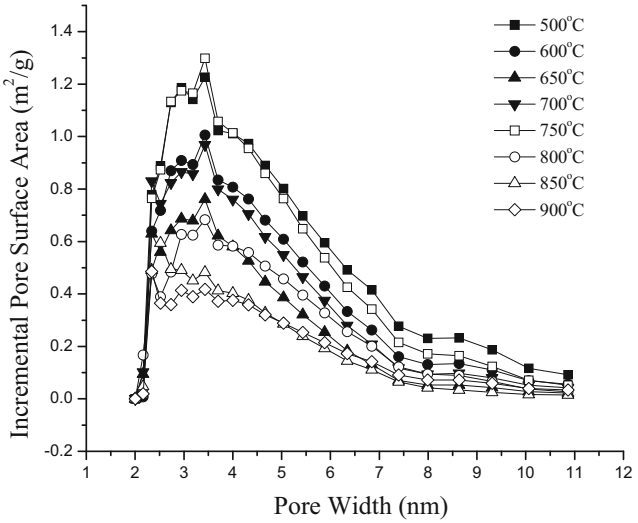

Fig. 12 Effect of pyrolysis temperature on the pore size distribution of activated carbons pyrolysed in nitrogen flow

The effects of the initial particle size of the oil-palm shells on the pore characteristics of the steam-activated carbons, pyrolysed in nitrogen flow and under vacuum, are shown in Figs. 9 and 10, respectively. Of the five particle size ranges tested, the 2–2.8-mm particle size range yielded the highest BET surface area, micropore surface area and total pore volume for both nitrogen flow and vacuum pyrolysis conditions. For the smallest particle size range of 1–2 mm, the ability to form an elaborate rudimentary pore network, due to its smaller physical volume constraint, is less favourable than the 2–2.8-mm size range, resulting in smaller pore development in the resulting activated carbon for the 1–2-mm size range when compared with the 2–2.8-mm size range. Increasing the particle size range beyond 2–2.8 mm decreased the BET surface area, micropore surface area and total pore volume of the activated carbons as shown in Figs. 9 and 10. The reasons are twofold. Firstly, increasing the particle size would increase the tortuosity path for the volatiles to move through the tiny and narrow pore passages from the particle interior to the particle surface for release during pyrolysis, thereby reducing the rudimentary pore development in the char. Secondly, increasing the particle size would reduce the accessibility and increase the tortuosity for the steam molecules to reach the internal pores of the char for the steam activation process. Hence, the initial particle size range of 2–2.8 mm was the optimum for the whole range of particle sizes tested.

Based on the parametric studies for oil-palm shells above, the optimum pyrolysis conditions were (i) pyrolysis temperature of 750 °C, hold time of 2 h, heating rate of 10 °C/min, nitrogen flow rate of 150 cm^3/min and initial particle size range of 2–2.8 mm for pyrolysis in nitrogen flow, and (ii) pyrolysis temperature of 675 °C, hold time of 2 h, heating rate of 10 °C/min and initial particle size range of 2–2.8 mm for pyrolysis under vacuum.

3.2 Surface morphology and pore size distributions of steam-activated carbons

The scanning electron micrographs in Fig. 11a and b show the surface morphology of the activated carbons pyrolysed in nitrogen and under vacuum, respectively. The pores of these two types of activated carbons are quite similar. The surfaces of the activated carbons show well-developed porous structures with well-defined regular pore sizes. The pore size distributions of the activated carbons pyrolysed in nitrogen flow at different pyrolysis temperatures are shown in Fig. 12. Only mesopore

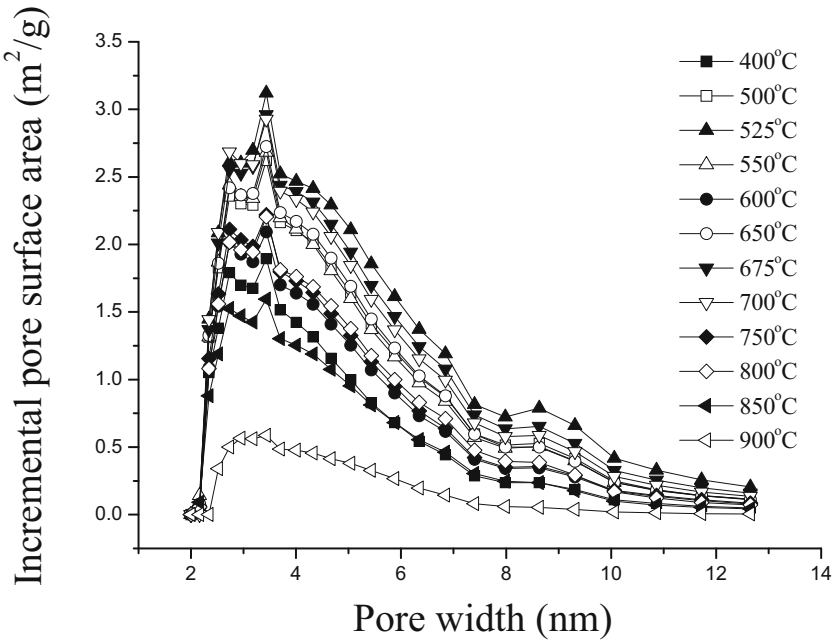

Fig. 13 Effect of pyrolysis temperature on the pore size distribution of activated carbons pyrolysed under vacuum

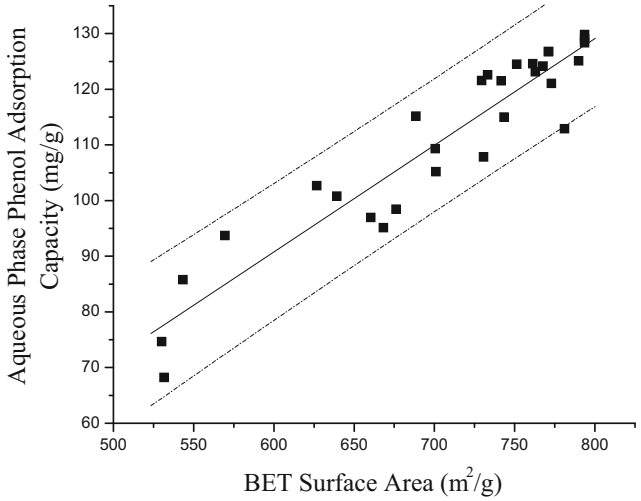

Fig. 14 Correlation between adsorption capacity and BET surface area for activated carbons pyrolysed in nitrogen flow

sizes are shown, and they ranged from 2 to 11 nm which are suitable for aqueous phase adsorption studies. From Fig. 2, the pyrolysis temperature of 750 °C yielded the largest BET surface area and it is confirmed here (Fig. 12) that it also yielded one of the two activated carbons with most pores for this size range. Similarly, the pyrolysis temperature of 900 °C yielding the smallest BET surface area (Fig. 2) correspondingly resulted in the least number of pores for this size range in Fig. 12. Figure 13 shows the pore size distributions of the activated carbons pyrolysed under vacuum at various pyrolysis temperatures for the mesopore size range of 2 to 12.7 nm. The pyrolysis temperature of 675 °C which yielded the largest BET surface area (Fig. 3) also produced one of the two activated carbons with most pores for this 2–12.7 nm size range. The activated carbon which had the smallest BET area at a pyrolysis temperature of 900 °C (Fig. 3) also showed the least number of pores for this size range of 2–12.7 nm in Fig. 13.

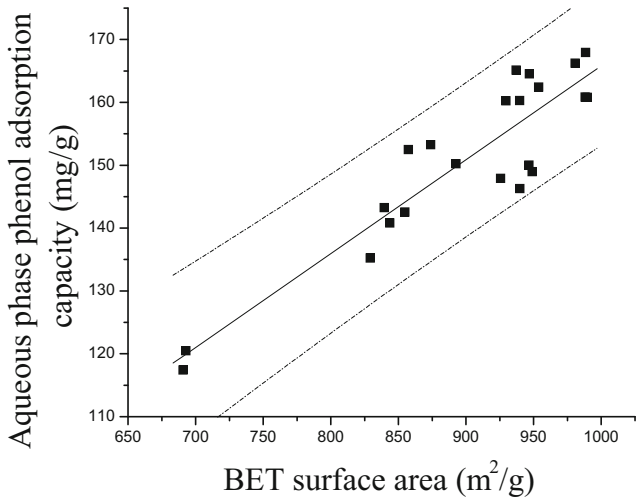

Fig. 15 Correlation between adsorption capacity and BET surface area for activated carbons pyrolysed under vacuum condition

An overall comparison of Figs. 12 and 13 would verify that the activated carbons prepared under vacuum pyrolysis conditions produced higher mesopore surface area for each pore size than those activated carbons prepared in nitrogen flow conditions for varying pyrolysis temperatures.

3.3 Aqueous phase phenol adsorption capacity of activated carbons

The effectiveness of the activated carbons as suitable adsorbents for aqueous applications was evaluated using phenol as the adsorbate. The adsorption capacity of the activated carbons to phenol was determined using an initial phenol concentration of 200 mg/l at 30 °C. To correlate the adsorption capacity and the pore characteristics, plots of the phenol adsorption capacity versus the BET surface area for all the activated carbons prepared are shown in Figs. 14 and 15 for activated carbons pyrolysed in nitrogen flow and under vacuum respectively. In Fig. 14, the adsorption capacity of phenol generally increased linearly with the BET surface area of the activated carbons pyrolysed in nitrogen flow. A regression line was drawn through the experimental data points, and its correlation coefficient was 0.93. The dashed lines shown indicated 95% confidence limits. The best adsorption result for this group of activated carbons was for the one with the highest BET surface area of 794 m^2/g yielding the largest adsorption capacity of 129 mg of phenol per g of activated carbon. In Fig. 15, the adsorption capacity of phenol also increased linearly with the BET surface area of the activated carbons pyrolysed under vacuum conditions and their correlation using linear regression resulted in a correlation coefficient of 0.94. The dashed lines also represented 95% confidence limits. Under vacuum pyrolysis, the best activated carbon yielded the highest BET surface area of 988 m^2/g and the largest adsorption capacity of 168 mg of phenol per g of activated carbon which is 30% more adsorption capacity than that for nitrogen pyrolysed activated carbon. By inference from the dependency of its BET surface by the pyrolysis operating parameters and initial shell particle, the phenol adsorption capacity of activated carbon is also dependent on the operating conditions during the pyrolysis of the char and the initial shell particle size.

4 Conclusions

Pyrolysis operating conditions and initial shell particle size have significant effects on the pore characteristics of the steam-activated carbons derived from oil-palm shells, which were either pyrolysed in a nitrogen stream or under vacuum. For both pyrolysis environments, the subsequent steam activation conditions were fixed at 900 °C, 1-h hold time and steam flow rate at 1.4 kg/h at a pressure of 2.1×10^5 N/m^2.

The optimum pyrolysis conditions were (i) pyrolysis temperature of 750 °C, hold time of 2 h, heating rate of 10 °C/min, nitrogen flow rate of 150 cm^3/min and initial particle size range of 2–2.8 mm for pyrolysis in nitrogen flow, and (ii) pyrolysis temperature of 675 °C, hold time of 2 h, heating rate of 10 °C/min and initial particle size range of 2–2.8 mm for pyrolysis under vacuum.

Under the nitrogen pyrolysis environment, the best activated carbon yielded the highest BET surface area of 794 m^2/g and achieved the largest adsorption capacity of 129 mg of phenol per g of activated carbon. Under the vacuum pyrolysis environment, the best activated carbon yielded the highest BET surface area of 988 m^2/g and achieved the largest adsorption capacity of 168 mg of phenol per g of activated carbon. The highest BET surface area and largest phenol adsorption capacity of the activated carbon pyrolysed under vacuum were respectively 24% and 30% greater than those for the activated carbon pyrolysed in nitrogen flow. Under vacuum pyrolysis, vaporization of the volatiles from the pore structure of the oil-palm shell structure advances to a lower pyrolysis temperature and more intense than the case of pyrolysis in the nitrogen flow, thereby yielding higher pore surface areas and total pore volume in the subsequent activated carbons.

Of all the pyrolysis parameters studied—pyrolysis temperature, hold time, heating rate (low heating rate region), nitrogen flow rate, initial particle size of the oil-palm shell and pyrolysis environment—the final pore characteristics of the steam-activated carbons are strongly dependent on the pyrolysis temperature, hold time, pyrolysis environment and initial particle size. The study also demonstrated that steam-activated carbon can be used to remove phenol, which is a waste product of industrial processes, from the aquatic ecosystems and water sources to protect aquatic species and humans from the harmful effects of phenol intakes.

Acknowledgements The author would like to thank Dr. Qipeng Jia for his assistance in the experimental work.

References

1. Guo J, Luo Y, Lua AC, Chi R, Chen Y, Bao X, Xiang S (2007) Adsorption of hydrogen sulphide (H_2S) by activated carbons derived from oil-palm shell. Carbon 45:330–336
2. Guo J, Lua AC (2000) Adsorption of sulfur dioxide onto activated carbons prepared from oil-palm shells impregnated with potassium hydroxide. J Chem Technol Biotechnol 75:971–976
3. Guo J, Xu WS, Chen YL, Lua AC (2005) Adsorption of NH_3 onto activated carbon prepared from palm shells impregnated with H_2SO_4. J Colloid Interface Sci 281:285–290
4. Zhao X, Zeng X, Qin Y, Li X, Zhu T, Tang X (2018) An experimental and theoretical study of the adsorption removal of toluene and chlorobenzene on coconut shell derived carbon. Chemosphere 206:285–292
5. Gonzalez-Garcia P (2018) Activated carbon from lignocellulosics precursors: a review of the synthesis methods, characterization techniques and applications. Renew Sust Energ Rev 82:1393–1414
6. Pereira MFR, Soares SF, Orfao JJM, Figueiredo JL (2003) Adsorption of dyes on activated carbons: influence of surface chemical groups. Carbon 41:811–821
7. Lua AC, Jia Q (2009) Adsorption of phenol by oil-palm-shell activated carbons in a fixed bed. Chem Eng J 150:455–461
8. Balci S, Dogu T, Yucel H (1994) Characterization of activated carbon produced from almond shell and hazelnut shell. J Chem Technol Biotechnol 60:419–426
9. Laine J, Yunes S (1992) Effect of the preparation method on the pore size distribution of activated carbon from coconut shell. Carbon 30:601–604
10. Gonzalez JF, Roman S, Encinar JM, Martinez G (2009) Pyrolysis of various biomass residues and char utilization for the production of activated carbons. J Anal Appl Pyrolysis 85:134–141
11. Uysal T, Duman G, Onal Y, Yasa I, Yanik J (2014) Production of activated carbon and fungicidal oil from peach stone by two-stage process. J Anal Appl Pyrolysis 108:47–55
12. Gergova K, Petrov N, Eser S (1994) Adsorption properties and microstructure of activated carbons produced from agricultural by-products by steam pyrolysis. Carbon 32:693–702
13. Rodriguez-Mirasol J, Cordero T, Rodriguez JJ (1993) Preparation and characterization of activated carbons from eucalyptus kraft lignin. Carbon 31:87–95
14. Lua AC, Yang T (2004) Effects of vacuum pyrolysis conditions on the characteristics of activated carbons derived from pistachio-nut shells. J Colloid Interface Sci 276:364–372
15. Wu H, Chen R, Du H, Zhang J, Shi L, Qin Y, Yue L, Wang J (2019) Synthesis of activated carbonfrom peanut shell as dye adsorbents for wastewater treatment. Adsorpt Sci Technol 37(1-2):34–48.
16. Foo KY, Hameed BH (2011) Preparation of activated carbon from date stones by microwave induced chemical activation: application for methylene blue adsorption. Chem Eng J 170:338–341
17. Lua AC, Guo J (1999) Chars pyrolyzed from oil palm wastes for activated carbon preparation. J Environ Eng 125(1):72–76
18. Lua AC, Lau FY, Guo J (2006) Influence of pyrolysis conditions on pore development of oil-palm-shell activated carbons. J Anal Appl Pyrolysis 76:96–102
19. Liu DD, Jia BY, Li S, Dong LJ, Gao JH, Qin YK (2019) Effect pf pyrolysis conditions on the improvement of the physicochemical structure of activated carbon obtained from Jixi bituminous coal. Asia Pac J Chem Eng 14:e2289. https://doi.org/10.1002/apj.2289
20. Guo J, Lua AC (2001) Kinetic study on pyrolytic process of oil-palm solid waste using two-step consecutive reaction model. Biomass Bioenergy 20:223–233